



ELSEVIER

Contents lists available at ScienceDirect

Applied Mathematical Modelling

journal homepage: www.elsevier.com/locate/apm

Practical application of empirical formulation of the stress concentration factor around equally sized dual spherical cavities to aluminum die cast



Sujit Bidhar^{a,*}, Osamu Kuwazuru^b, Yoshinori Shiihara^c, Yoshihiko Hangai^d,
Takao Utsunomiya^e, Ikumu Watanabe^a, Nobuhiro Yoshikawa^c

^a National Institute for Material Science, Research Center for Strategic Material Unit, Sengen 1-2-1 Tsukuba, Ibaraki 305-0047, Japan

^b Department of Nuclear Power and Energy Safety, University of Fukui, 3-9-1 Bunkyo, Fukui-shi, Fukui 910-8507, Japan

^c Institute of Industrial Science, The University of Tokyo, 4-6-1 Komaba, Meguro, Tokyo 153-8505, Japan

^d Department of Mechanical System Engineering, Gunma University, 1-5-1 Tenjin-cho, Kiryu-shi, Gunma 376-8515, Japan

^e Research Organization of Advanced Engineering, Shibaura Institute of Technology, 307 Fukasaku, Minuma-ku, Saitama-shi, Saitama 337-8570, Japan

ARTICLE INFO

Article history:

Received 15 January 2013

Received in revised form 4 July 2014

Accepted 10 July 2014

Available online 22 July 2014

Keywords:

Finite element method

Stress concentration

Porosity

Dual cavity

Aluminum die cast

ABSTRACT

An empirical method is developed for obtaining the stress concentration factor for a pair of equally sized spherical cavities embedded in a large continuum in three-dimensional space. For practical applications such as die-cast materials containing many pores, we construct a simple and robust closed-form equation to evaluate the stress concentration factor considering the interaction between two cavities. The stress concentration factor can be used to evaluate the effect of pores on the material strength and the probable location of pores that will initiate a fatigue crack. Three-dimensional finite element linear elastic analysis was carried out to evaluate the stress concentration factors for arbitrary locations of the two cavities. The effects of the inter-cavity distance and the orientation of the inter-cavity axis with respect to the loading direction on the stress concentration factor are numerically obtained by systematically changing each of these parameters. Two empirical equations are proposed to fit the stress concentration factor data calculated by finite element analysis after considering various boundary conditions from a mechanical standpoint, and the parameters of the empirical formula are obtained by non-linear curve fitting with regression analysis.

© 2014 Elsevier Inc. All rights reserved.

1. Introduction

The stress enhancement caused by inter-cavity interaction is very important from a fatigue strength point of view, since it facilitates fatigue crack initiation [1,2] and degrades the long-term reliability of metal members under dynamic loading. Cavities of irregular shape and size are usually formed during manufacturing, but evaluating the stress field around an irregular boundary is difficult, and closed-form solutions are not available for such geometries. For simplicity, such voids

* Corresponding author.

E-mail addresses: sujit@telu.iis.u-tokyo.ac.jp (S. Bidhar), kuwa@u-fukui.ac.jp (O. Kuwazuru), nori@telu.iis.u-tokyo.ac.jp (Y. Shiihara), hanhan@gunma-u.ac.jp (Y. Hangai), utunomiya@sic.shibaura-it.ac.jp (T. Utsunomiya), WATANABE.Ikumu@nims.go.jp (I. Watanabe), yoshi@telu.iis.u-tokyo.ac.jp (N. Yoshikawa).

are assumed to be regular spherical cavities. Therefore, it is important to study the interference between stress fields caused by multiple spherical cavities. If these inter-cavity interactions can be modeled using simple mathematical functions, the models may find practical application in structural materials such as pressure die cast aluminum alloys in which microporosity is inherent to the casting process. Aluminum die cast materials are widely used in the automotive industry. The fatigue performance of these components is greatly influenced by the presence of cavities [3–7]. Therefore, modeling the three-dimensional stress field around a spherical cavity pair would help identify the stress concentrated regions in actual die cast materials containing many cavities in the form of gas pores and shrinkage pores.

An aluminum die cast part contains a large number of gas pores of irregular shape and size. It would be extremely difficult to consider the interactions among all of the pores at once. A good first step, however, would be to evaluate an empirical function representing the stress concentration factor for a pair of ideal spherical cavities of the same size. Then, this function can be modified to approximate stress concentrations around irregularly shaped cavities. Therefore, in this study, a systematic numerical evaluation of the stress concentration factor for a pair of spherical cavities in three dimensions is carried out. Many researchers have dealt with the problem of a single spherical cavity in an infinite solid by using spheroidal harmonics [8]. Several other numerical methods have been suggested to solve the problem of an infinite solid containing a pair of cavities or inclusions [9–15]. Usually, such methods employ complex stress functions and series of bi-spherical harmonics or multi-pore expansions to describe the stress field around a pair of cavities [9–12]. Stenberg and Sadowsky used Papcovich–Boussinesq displacement functions in spherical dipolar coordinates to solve for the stress distribution around a spherical cavity pair in an infinite solid [9]. Miyamoto et al. [12,13] used spherical coordinates and Papkovitch–Neuber stress functions. Such mathematical functions often involve infinite series, which demands more computation time to evaluate the various coefficients. Accuracy is often affected by the number of terms selected in the infinite series. Convergence is not guaranteed when the inter-cavity distance is small [14,15]. Analytical solutions are also unavailable for differently sized cavity pairs and asymmetrical geometries, such as when the inter-cavity axis is not perpendicular to the loading direction. Therefore, in this paper, we attempted to develop an empirical formula for a pair of spherical cavities based on the numerical results of finite element analyses. Parametric studies are then made for a spherical cavity pair by systematically changing both the orientation of the inter-cavity axis with respect to the loading direction and the inter-cavity distance. A similar work is also done to describe stress concentration factor as a function of pore parameters using a simple power function [16]. In this paper we show two types of formula for the function expressing the effect of distance of two pores. One is a simple power function [16], and the other is a comprehensive double exponential function. The difference between two formulae and their accuracy is discussed. We have enhanced the accuracy by using a double exponential function for the effect of distance. The parameters of the empirical formula are optimized through exclusive and coupled search. The practical significance of both empirical formulae, *i.e.*, double exponential function and power function, are discussed in order to provide a qualitative guide line to industry personnel for setting an acceptance limit to die cast parts.

2. Methodology

2.1. Equal size dual cavity problem

Two spherical cavities of equal size are introduced into a large solid cylindrical continuum. The radius and height of the cylindrical volume are forty times the cavity diameter, in order to avoid any free boundary effect. Fig. 1 shows a cross-sectional

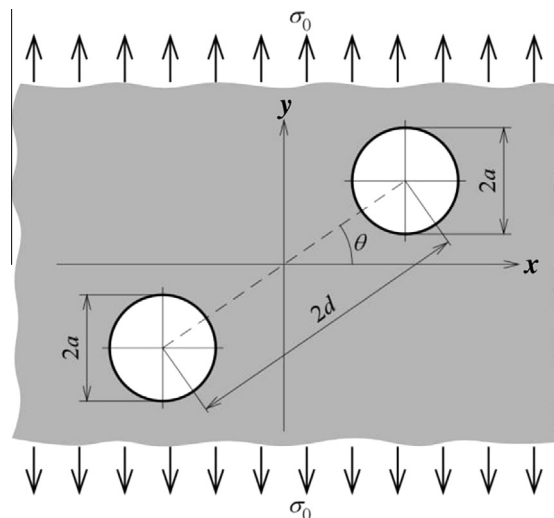


Fig. 1. Layout of a pair of identical spherical cavities in an infinite continuum.

view of a pair of such cavities. $2d$ denotes the distance between cavity centers, $2a$ is the cavity diameter, and θ is the orientation of the inter-cavity axis with respect to the plane normal to the loading direction. As the stress concentration is well described by radial distance normalized by radius for a single spherical cavity case, the inter-cavity distance is normalized by introducing a parameter δ representing the ratio between the inter-cavity distance ($2d$) and the diameter ($2a$). δ and θ are varied systematically from 1.005 to 2 and 0° to 90° , respectively. A far field stress of σ_o is applied in the y -direction.

2.2. Expression for stress concentration factor

Three-dimensional finite element linear elastic analysis is carried out, and the maximum principal stress $\sigma_{1\max}$ is evaluated in each case. The stress concentration factor K_t is defined as the ratio of the maximum principal stress to the applied nominal stress, as $K_t = \sigma_{1\max}/\sigma_o$. K_t is evaluated for different values of non-dimensional distance δ and orientation angle θ . The value of K_t can be thought to be comprised of two parts: K_{iso} , which is the stress concentration due to a single isolated cavity and K_{int} , which results from interaction between the cavities.

$$K_t = K_{\text{iso}} + K_{\text{int}} \quad (1)$$

In the above equation, K_t is taken as a linear combination of K_{iso} and K_{int} because it is believed that the overall stress distribution due to the dual cavity interaction can be obtained approximately by superimposing the stress distributions caused by the individual cavities. It is also believed that under certain extreme conditions, the K_t value for a dual cavity system will reduce to a constant value of K_{iso} .

2.3. Auto meshing procedure

Finite element analysis is carried out by ANSYS. One important aspect of the finite element method is mesh generation. For this purpose, ANSYS ICEMCFD is used to generate an unstructured volume mesh for the entire continuum containing the cavities. The cylindrical continuum is large enough to simulate the cavities in an infinite volume. 10-node tetrahedral elements are used. To guarantee convergence, the mesh is refined and optimized using geometrical refinement techniques and the curvature-based refinement algorithm of the ANSYS ICEMCFD mesh module to obtain a very fine mesh near the cavities and a relatively coarse mesh in regions more distant from the cavities. The minimum size of the element is tentatively set to $0.5 \mu\text{m}$. In the curvature-based refinement technique [17], forty elements are chosen around the curvature and five elements are chosen in the gap between the cavities. This ensures that even at close proximity to the cavities there will be at least five tetrahedral elements between their boundaries to obtain smooth stress variation in that region. Usually, geometry containing discontinuity results in distorted elements with high aspect ratios in order to achieve the required element size and quantity according to the parameters set in the curvature-based refinement. For example, when the distance between the cavities is too small, the elements must be squeezed in order to fit five of them into the gap between the cavities, resulting in a high aspect ratio. Therefore, a smoothing technique is also employed by setting the smoothing iteration parameter to five and the aspect ratio parameter close to one. In each smoothing iteration, elements are reoriented and re-meshed so that high aspect ratio elements are replaced with elements of the desired aspect ratio, as indicated by the aspect ratio parameter. This operation is carried out five times, and as a result, the distorted elements with high aspect ratios are replaced automatically by subsequent meshing iteration until the aspect ratio improves. Multiple nodes formed at the same position are also merged. Fig. 2(a) shows a cross-sectional view of one such mesh pattern thus obtained around the cavities and Fig. 2(b) highlights the fine mesh in the gap between the two cavities with five elements. A total of about one hundred thousand tetrahedral elements are created. As the relative size of the mesh compared to the region between the cavities affects the stress values, a consistent mesh refinement procedure is adopted for all cases involving various values of δ and θ . As a result, more elements are formed when the region between the cavities are small, and tetrahedral elements as small as $0.002a$ are formed.

2.4. Validation for a single spherical cavity

To validate the auto-meshing procedure, the accuracy of the stress obtained from the finite element analysis with an automatically generated mesh is examined by comparing it with the analytical solution of the single spherical cavity problem. Analytical solutions are available for evaluating the stress distribution around a spherical cavity in an infinite solid [1]. Following the work of Goodier [18], Timoshenko [19] found an analytical solution for a single spherical cavity under uniaxial tension at infinity by using a complex stress function and superposition theory. A spherical cavity of radius a is considered. A far field tensile stress of σ_o is applied in the y -direction, as shown in Fig. 3. The stress distribution in an equatorial plane in the radial direction is given by Eq. (2),

$$\frac{\sigma_y}{\sigma_o} = 1 + \frac{4 - 5\nu}{2(7 - 5\nu)} \left(\frac{a}{r}\right)^3 + \frac{9}{2(7 - 5\nu)} \left(\frac{a}{r}\right)^5, \quad (2)$$

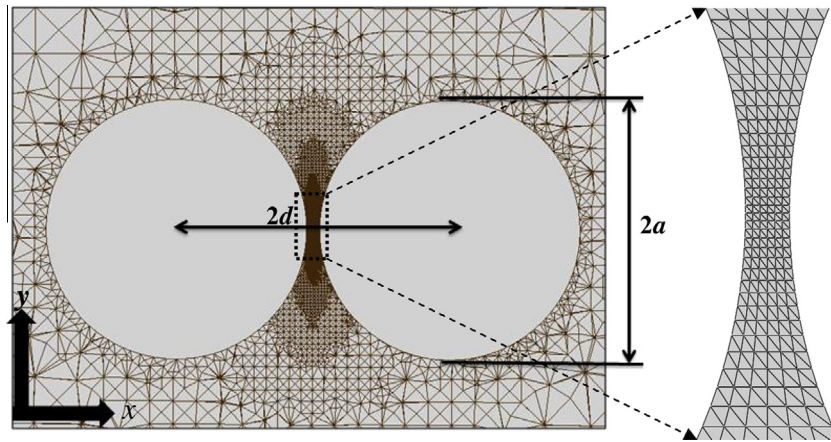


Fig. 2. (a) Cross-sectional plane showing an optimized mesh around the spherical cavities. (b) Zoomed section of mesh pattern between the spherical cavities.

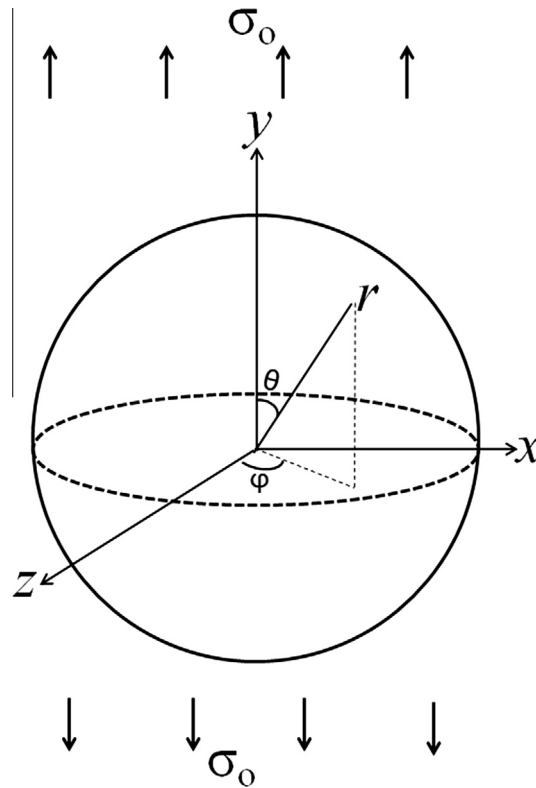


Fig. 3. Single spherical cavity loaded by a far field tensile stress.

where r is the radial distance from the center of the sphere in the equatorial plane. ν is Poisson's ratio, which is taken to be 0.3 in the present case. Li et al. [20] also developed an analytical solution by considering more realistic material properties and using spherical harmonic functions.

Three-dimensional finite element analysis is carried out for the single spherical cavity embedded in a large continuum with a uniform tensile stress applied to the large continuum in the y -direction while the lower portion of the continuum is fixed. The mechanical properties of aluminum die cast alloy are used in the finite element linear elastic stress analysis. The finite element model is automatically generated by the auto meshing technique described above. A Young's modulus of 76 GPa and a Poisson's ratio of 0.3 are used. The distribution of normalized stress σ_y/σ_0 in the equatorial plane is plotted in the normalized radial distance from the cavity surface, in order to account for variation in cavity size. This is plotted in Fig. 4 along with the analytical solution of Eq. (2). The ratio r/a on the x -axis is the distance from the edge of the cavity

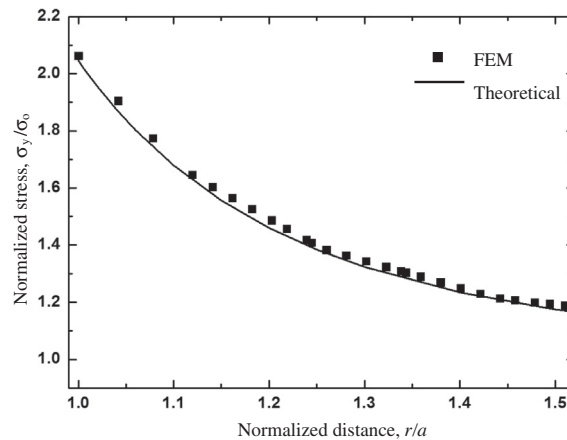


Fig. 4. Comparison of finite element analysis and analytical solution for a single spherical cavity.

on the equatorial plane normalized over the radius of the cavity. As can be seen from Fig. 4, there is good agreement between the three-dimensional stress distribution calculated by finite element analysis and the analytical solution.

3. Finite element results for a dual cavity system

A tensile stress of $\sigma_0 = 10$ MPa is applied in the y -direction to the top surface of the large cylinder far from the cavities, and the bottom surface of the cylinder is fixed. Assuming an aluminum alloy, a Young's modulus of 76 GPa and a Poisson's ratio of 0.3 are used as material properties. The non-dimensional distance δ is varied from 1.005 to 2 for various values of θ ranging from 0° to 90° , and selected results are listed in Table 1. It can be seen that for the value of $\delta = 2$, K_t converges to a constant value of 2.104, irrespective of orientation angle θ . This means that the presence of another cavity at that distance has no effect on the stress concentration K_t . Therefore, K_t can be treated as a constant and denoted as K_{iso} . The slight discrepancies between theoretical and calculated K_{iso} values can be attributed to errors arising from the numerical computation. The finite element result in Fig. 4 for K_{iso} is found to be 2.062, which is slightly higher than the theoretical value of 2.046 [21,22]. This is due to the fact that the finite element values are computed on the gauss points of the elements, which are slightly offset from the actual cavity boundary. So, for our empirical formulation, the theoretical value of $K_{iso} = 2.046$ is taken for accuracy. For θ values greater than 50° , there is less interaction between the cavities. As can be seen from data in Table 1 and Fig. 5, for small distances of separation between the cavities and a δ of less than 1.1, K_t is very sensitive to the orientation angle θ . K_t decreases rapidly as the orientation angle increases, up to 60° . For orientation angles above 60° , K_t approaches the value corresponding to that of a single isolated spherical cavity. Thus, the distance of separation between the cavities has a minimal effect on K_t for higher orientation angles. The threshold orientation angle seems to be somewhere between 50° and 60° , beyond which the normalized distance has a negligible effect. In other words, for orientation angles less than 50° , there is a sharp increase in K_t (more interaction) within certain threshold values of normalized distance δ less than 1.2. As can be seen in Fig. 5, for low orientation angles below 45° , the high-stress zone completely lies within the region along the line joining the centers of the two cavities. Beyond an orientation angle of 45° , the maximum principal stress as well as the maximum stressed region shifted away from the inter-cavity region to the individual equatorial planes. For a 90° orientation, the maximum stressed region appears near the equatorial planes of the individual cavities, and not between the regions connecting their centers, similar to the stress distribution of a single isolated cavity. Fig. 5 shows this gradual variation of stress distribution with orientation angle when δ is fixed at 1.04. For a 90° orientation, the value of K_t decreases below that of an individual cavity at small separation distances. This may be because the stress concentration around individual cavities is relaxed by a small amount when the two cavities come very close to each other, so that the overall geometry of the dual cavity system takes an ellipsoidal shape with loading along the major axis. Fig. 5(f) shows the distribution of stress on a line between the cavities on the equatorial plane joining the cavities boundaries, for different values of δ and for inter-cavity axis normal to loading direction ($\theta = 0^\circ$). A path is defined in ANSYS by choosing two points close to the edges of the two cavities on the equatorial plane. The principal stress is plotted along this path. A number of such paths were drawn for cavities at different distances ranging from $2.5 \mu\text{m}$ to $100 \mu\text{m}$. The abscissa is normalized by the distance of separation. In the graphs in Fig. 5(f), the position "0" refers to the midpoint of the region of separation along the inter-cavity axis. The position "-1" corresponds to the edge of the cavity on left, while the position "+1" refers to the edge of cavity on right. The distribution of stress is symmetric, decreasing away from one cavity, reaching its minimum at the middle of the path, and reaching its maximum as it approaches the next cavity.

Table 1
Finite element computed results of stress concentration factors K_t for various δ and θ .

δ	Orientation angle, θ							
	0°	20°	30°	40°	45°	50°	60°	90°
1.0050	9.1372	7.8650	6.5419	5.0536	4.2170	3.3519	2.1802	1.9882
1.0100	6.9827	6.0289	5.2504	4.0170	3.3793	2.7346	2.1582	1.9261
1.0200	5.3557	4.7115	4.1727	3.2804	2.8561	2.3143	2.1069	1.9386
1.0400	4.1166	3.7903	3.3866	2.7145	2.3672	2.1450	2.0688	1.9051
1.0600	3.5608	3.3912	2.9996	2.4793	2.2161	2.1423	2.0872	1.9288
1.1000	3.0223	2.9421	2.7129	2.3183	2.1165	2.1395	2.0775	1.9163
1.2000	2.4312	2.4553	2.4599	2.1815	2.1110	2.1083	2.0937	1.9421
1.3000	2.4025	2.3023	2.4918	2.1382	2.1067	2.1089	2.0866	1.9414
1.4000	2.1445	2.3721	2.3736	2.1394	2.1458	2.0945	2.0821	1.9627
2.0000	2.1584	2.1580	2.1580	2.1580	2.1580	2.1580	2.1580	2.1580

4. Empirical formulation of the stress concentration factor

K_{iso} in Eq. (1) is taken as the linear elastic theoretical value of 2.046 corresponding to the stress concentration factor of a single isolated spherical cavity in an infinite continuum. K_{iso} is found to be 2.046 for a Poisson's ratio of 0.3 [21,22]. Table 1 lists the finite element results for K_t for various values of δ and θ . As can be seen from these data, since K_{iso} is set to a constant value, the K_{int} term is affected simultaneously by the non-dimensional parameter δ and the orientation angle θ . Therefore, a mathematical function for K_{int} should contain both δ and θ . At constant values of δ , K_{int} varies with orientation angle θ , and vice versa. Therefore, we can write the function as a combination of two functions, each containing one of these individual parameters. Thus, we assume K_{int} in variable separation form as follows,

$$K_{\text{int}} = \alpha(\theta)F(\delta). \quad (3)$$

The fitting curves are expected to be of highly non-linear in nature. Finding suitable initial values for the parameters for such curves is crucial. So in the first step, an exclusive curve fitting is performed for the functions $\alpha(\theta)$ and $F(\delta)$ to obtain the initial values of the parameters which are then optimized using a coupled curve fitting method.

4.1. Curve fitting through exclusive search

Appropriate mathematical functions for $\alpha(\theta)$ and $F(\delta)$ are chosen and their parameters are found by fitting against the numerical results of Table 1.

4.1.1. K_{int} variation with orientation angle θ

For constant values of δ , the data seem to follow a cosine function with orientation angle θ . Considering the periodicity of K_{int} with respect to θ , a general cosine function for $\alpha(\theta)$ is chosen in Eq. (3) as,

$$K_{\text{int}} = (\cos^2\theta)^\xi F(\delta). \quad (4)$$

In the above equation, $F(\delta)$ is treated as a parameter independent of θ . The initial guess of Eq. (4) as power function of $\cos\theta$ is made by plotting the finite element data over the entire range of θ from 0° to 90° for each δ and observing the trend. Introducing a cosine function satisfies the boundary condition at $\theta = 90^\circ$; that is, the stress concentration factor should approach that of a single cavity when the orientation angle $\theta = 90^\circ$ for large δ . From the geometry of the dual cavity system, the stress concentration factors for $90^\circ \leq \theta \leq 180^\circ$ should be a mirror image of that for $0^\circ \leq \theta \leq 90^\circ$. Mathematically, this is achieved by taking the square of $\cos\theta$. Since $\cos^2\theta$ has a periodicity of 180°, it also satisfies the symmetry of the geometry; that is, the stress concentration factor should remain the same if the cavities are exchanged along the line joining their centers. The computed data does not exactly follow $\cos^2\theta$, but rather die out quickly after 50°. To take this into account, the index ξ is introduced in Eq. (4) and fitted against the finite element results listed in Table 1. Fig. 6 shows the goodness of this fitted function in Eq. (4) in terms of K_t i.e. $K_t = K_{\text{int}} + 2.046$, since only K_t is available from FEM. The values of the parameters in Eq. (4), $F(\delta)$ and ξ , are found by regression analysis for each δ , and are listed in Table 2. The values of coefficient of determination, R^2 [23,24] listed in Table 2 quantify how well the chosen function fits to computed data. R^2 values closer to 1 suggest a better fit.

4.1.2. K_{int} variation with normalized distance δ

To find a suitable fitting function for $F(\delta)$, two candidate functions are chosen. One is a single power function [16], and the other is a double exponential function.

4.1.2.1. Single power function for $F(\delta)$. For constant orientation angle θ , the data is fitted to follow a power law function in δ as given below,

$$K_{\text{int}} = \alpha(\theta)(\delta - 1)^{-\eta}. \quad (5)$$

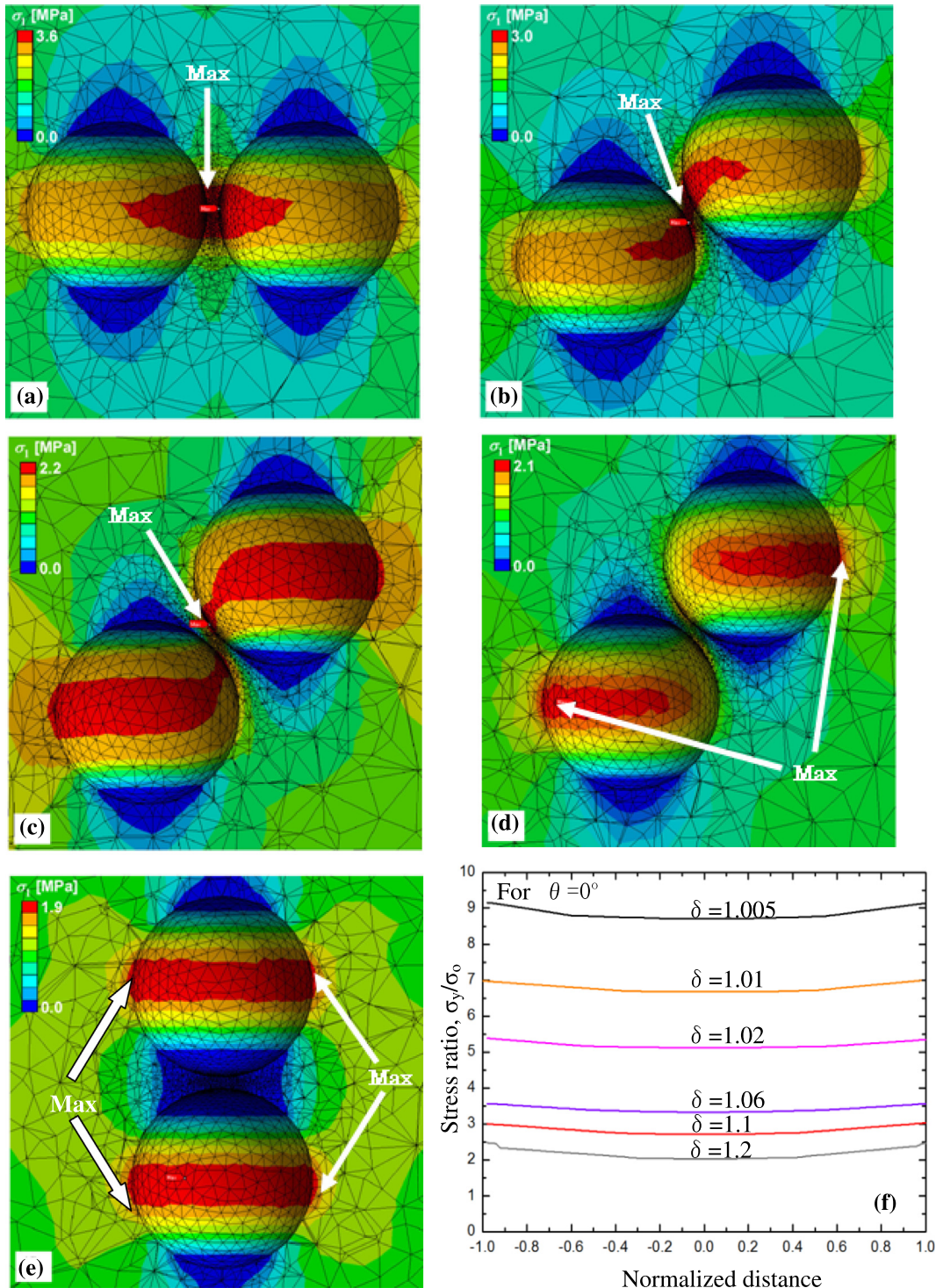


Fig. 5. Dependence of the maximum principal stress location on the angle between the inter-cavity axis and the loading direction at $\delta = 1.04$. (a) $\theta = 0^\circ$, (b) $\theta = 30^\circ$, (c) $\theta = 45^\circ$, (d) $\theta = 50^\circ$, (e) $\theta = 90^\circ$, (f) stress distribution along the equatorial plane between the spherical cavities.

η is always a positive number. The validity of the above equation is tested for various boundary conditions. As the distance of separation between the cavities approaches zero, δ approaches one, and the elastic stress concentration factor should approach infinity. Mathematically, this is achieved by the presence of a negative exponent of $F(\delta)$, which would make

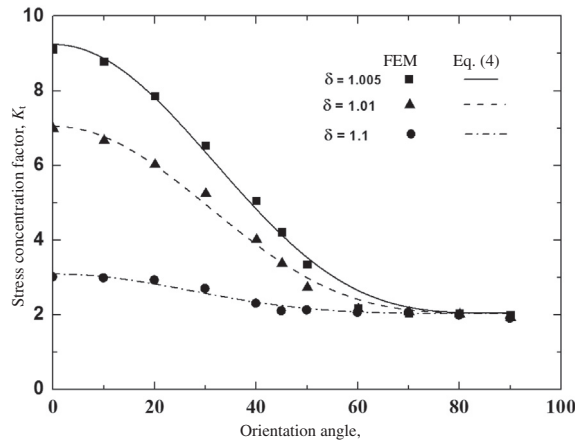


Fig. 6. Curve fitting by Eq. (4) showing variation of K_t with changing inter-cavity axis orientation – exclusive function fitting.

Table 2
Parameters of Eq. (4) obtained by regression analysis –exclusive search.

δ	$F(\delta)$	ξ	R^2
1.005	6.869	1.784	0.978
1.01	5.007	1.887	0.993
1.02	3.375	2.032	0.989
1.04	2.174	2.285	0.981
1.06	1.621	2.397	0.978
1.10	1.054	2.344	0.960
1.15	0.701	2.068	0.919
1.20	0.464	1.798	0.891
1.30	0.417	1.813	0.807
1.40	0.236	1.064	0.625

$F(\delta)$ approach infinity as δ approaches one, thus causing K_t to approach infinity. Eq. (5) satisfies this boundary condition. The other condition is that for large separation distances between the cavities, there should be no interaction of stress perturbations created by individual cavities, since these perturbations die out quickly after reaching a finite distance from the cavity. Therefore, the stress concentration factor for such a pair of cavities should approach that of a single cavity. For large inter-cavity distances, δ approaches infinity, causing $F(\delta)$ to approach zero and reducing K_t to K_{iso} . The chosen function satisfies both of these boundary conditions.

Considering $\alpha(\theta)$ as a parameter independent of δ for a particular orientation angle θ , Eq. (5) is fitted against the computed finite element results. Fig. 7 shows the goodness of the resulting power function to the computed data of K_t evaluated by finite element method over normalized distance δ for various orientation angles θ . By regression analysis, the values of index η and $\alpha(\theta)$ are found in each case, and are listed in Table 3.

4.1.2.2. Double exponential function for $F(\delta)$. For fixed values of θ in Table 1, K_t is fitted over δ by choosing a double exponential function for $F(\delta)$ in Eq. (3) as follows,

$$K_{int} = \alpha(\theta) \left[B_1 \exp \left\{ -\frac{(\delta - 1)}{t_1} \right\} + B_2 \exp \left\{ -\frac{(\delta - 1)}{t_2} \right\} \right]. \tag{6}$$

The above equation satisfies the condition for a large separation of cavities, for which K_t approaches K_{iso} as δ approaches infinity. The negative exponent ensures that $F(\delta)$ vanishes as δ approaches infinity. Unlike the single power function, however, the double exponential function does not yield an infinite stress concentration for a very close proximity of cavities. Instead, it converges to a finite value that is too high to actually occur in practical situations, because the material will yield at some lower stress value.

Considering $\alpha(\theta)$ as a parameter independent of δ , for a particular orientation angle θ , Eq. (6) is fitted against the finite element results. Fig. 8 shows the goodness of this fitted double exponential function against the finite element analysis results for K_t over normalized distance δ for various orientation angles θ . By regression analysis, the values of $\alpha(\theta)$ and other parameters are found for each case, and are listed in Table 4.

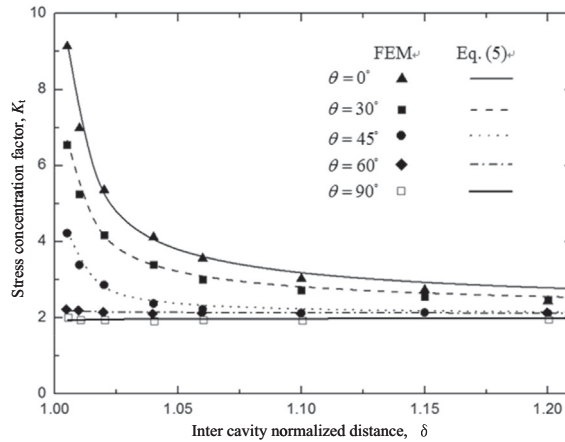


Fig. 7. Power function fitting of stress concentration variation with normalized inter-cavity distance – exclusive function fitting.

Table 3
Parameters of Eq. (5) obtained by regression analysis –exclusive search.

θ	$\alpha(\theta)$	η	R^2
0°	0.220	0.663	0.987
10°	0.241	0.634	0.993
20°	0.222	0.620	0.995
30°	0.190	0.602	0.995
40°	0.064	0.731	0.994
45°	0.026	0.842	0.986
50°	0.006	1.013	0.981
60°	0.030	0.249	0.261
80°	-0.112	0.241	0.082
90°	-0.058	0.145	0.136

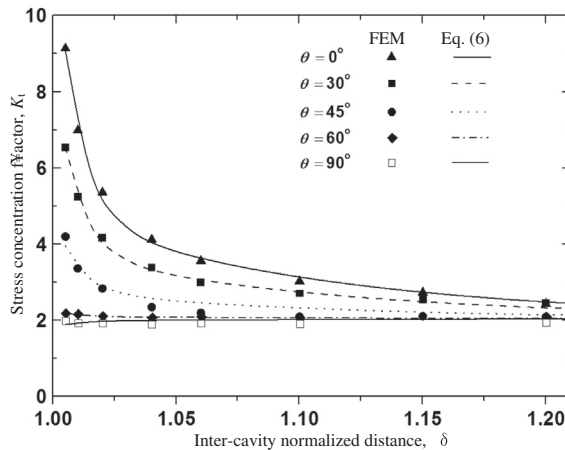


Fig. 8. Double exponential function fitting of stress concentration variation with normalized inter-cavity distance – exclusive function fitting.

4.2. Curve fitting through coupled search

From the R^2 values listed in Table 3, it can be seen that, although Eq. (5) fits the finite element data excellently, the index η in Eq. (5) is dependent on the orientation angle θ . A similar observation can be made in Table 2 for Eq. (4) and the dependence of index ζ on normalized inter-cavity distance δ . As a result, the functions described in Eqs. (4) and (5) are not mutually exclusive. Therefore, it is required to find the parameters of these equations as mutually independent of each other *i.e.*, the value of η and ζ should be constant for all δ and θ . In order to achieve the optimum values for the parameters, it is required to simultaneously solve the coupled function of $\alpha(\theta)$ and $F(\delta)$.

Table 4
Parameters of Eq. (6) obtained by regression analysis- exclusive search.

θ	$\alpha(\theta)$	B_1	B_2	t_1	t_2	R^2
0°	1.5440	4.8600	1.7600	0.0095	0.1095	0.9948
10°	1.1677	6.3039	2.2526	0.0088	0.1111	0.9936
20°	1.1073	5.8129	2.0837	0.0085	0.1177	0.9939
30°	0.9328	5.1929	1.1514	0.0136	0.2708	0.9907
40°	0.8513	4.2430	1.0540	0.0094	0.0952	0.9924
45°	0.8100	4.2300	2.176	0.0032	0.0249	0.9864
50°	0.5900	4.1032	0.1316	0.0073	0.1000	0.9548
60°	0.2394	0.0010	0.7378	0.0001	0.0200	-1.4691
70°	0.1000	0.1000	0.1838	0.1000	0.1000	-1.5491
80°	0.0127	0.1000	0.0788	0.0001	0.0001	-1.1500
90°	0.0347	0.0001	0.2079	0.0001	0.0001	-3.5160

4.2.1. Cosine – power function

The parameters η and ξ , are found by introducing Eqs. (4) and (5) into Eq. (3) and solving it by taking the initial values of these parameters obtained in exclusive approach of previous as follows,

$$K_{\text{int}} = A(\cos^2 \theta)^\xi (\delta - 1)^{-\eta}. \quad (7)$$

The combined effect of orientation angle and cavity separation distance can now be evaluated by the above empirical equation. The constants in Eq. (7) are evaluated by surface fitting the values of K_t over δ and θ simultaneously, in two dimensions. The constants are evaluated by regression analysis, with the following results,

$$A = 0.246, \quad \xi = 1.868, \quad \eta = 0.644. \quad (8)$$

The model fits the set of data given in Table 1 with a R^2 value of 0.988. The value of R^2 closer to 1 suggests the proposed equation fits the computed data with the minimum error. Fig. 8 shows a fitted surface plot of Eq. (7) against the computed values from finite element analysis with variation of stress concentration factor K_t over inter-cavity normalized distance δ and orientation angle θ .

4.2.2. Cosine – exponential function

In order to consider the combined effect of the angle of orientation and distance of separation between the cavities, the double exponential function for $F(\delta)$ and the cosine power function $\alpha(\theta)$ are introduced simultaneously into Eq. (3) as follows (Fig. 9),

$$K_{\text{int}} = A(\cos^2 \theta)^\xi \left[B_1 \exp \left\{ -\frac{(\delta - 1)}{t_1} \right\} + B_2 \exp \left\{ -\frac{(\delta - 1)}{t_2} \right\} \right]. \quad (9)$$

Non-linear surface fitting is carried out for the above function over δ and θ axes against the computed finite element data for K_t listed in Table 1, and the parameters of Eq. (9) are evaluated by regression analysis as follows,

$$A = 0.945, \quad \xi = 1.878, \quad B_1 = 3.07, \quad B_2 = 1.0, \quad t_1 = 0.0095, \quad t_2 = 0.12048. \quad (10)$$

The empirical formula given in Eq. (9) fits the computed data with $R^2 = 0.9897$. Fig. 10 shows a fitted surface plot of Eq. (9) against the computed values of K_t by finite element analysis for variation of stress concentration factor over inter-cavity normalized distance δ and orientation angle θ .

The R^2 values in Tables 3 and 4 are lower for higher orientation angles because these values are calculated from a relative error that is a ratio between a regression sum of squares (S_{reg}) and sample variance (S_{tot}), and is defined as $R^2 = 1 - S_{\text{reg}}/S_{\text{tot}}$ [24]. Therefore, if sample variance is lower, as in the case of higher orientation angles, R^2 will have a low value, even though S_{reg} is small.

5. Discussion

The empirical formulae presented in Eqs. (7) and (9) are simple in structure and do not involve complicated mathematical formulations or series that demand substantial computational effort. In previous research involving the stress fields around dual cavity systems, evaluation of the stress concentration factor would involve finding a solution to complex stress or displacement functions using power series, spherical harmonics, or other expansion series involving many parameters [9–12]. Furthermore, convergence would not always be guaranteed. In contrast, the empirical formulation presented in this paper has few parameters, requiring the user to simply input the inter-cavity distance and the orientation angle. Evaluation of the stress concentration factor is straightforward and fast. There is no issue with convergence, as the evaluation does not involve iteration.

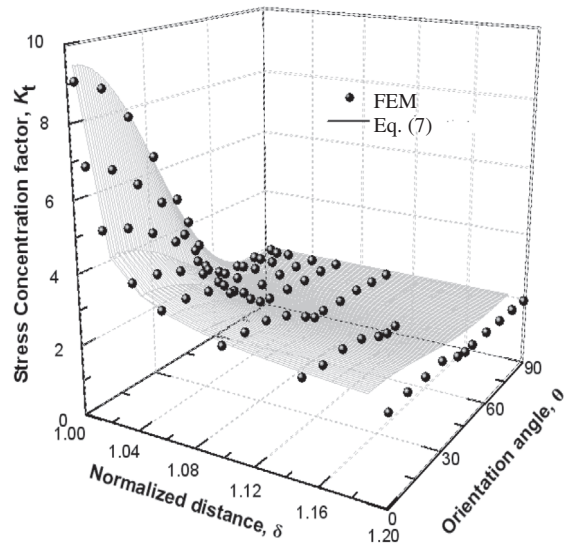


Fig. 9. Simultaneous cosine-power function fitting of stress concentration variation with normalized inter-cavity distance and orientation angle – coupled function fitting.

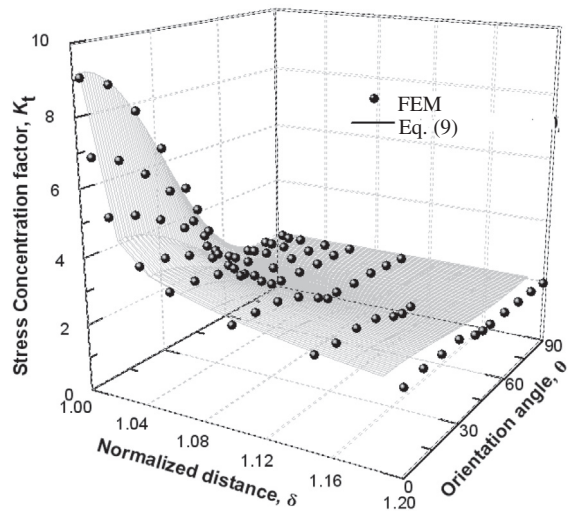


Fig. 10. Simultaneous cosine-double exponential function fitting of stress concentration variation with normalized inter-cavity distance and orientation angle – coupled function fitting.

The primary limitation of empirical formulation is that it is not possible to obtain the entire stress distribution around the cavities, but rather the method predicts only the maximum stress value. However, in many practical engineering design problems, evaluation of the maximum stress is critical. For example, the empirical formulation is applicable for components containing gas pores such as aluminum die castings in which the local stress concentration factor plays an important role in determining fatigue life [3].

In the automotive industry, pressure die casting introduces micro-porosity of nearly spherical shape in many components. Evaluation of the maximum stress is more practical for industrial use to cope with fatigue life prediction than detail stress distribution due to presence of such cavities. An easy, reliable method of obtaining the maximum stress is highly useful, since this would enable fatigue life prediction. Information regarding pore size, location, and orientation are usually obtained from X-ray CT images or optical micrographs of sample cross-sections. Therefore, in this situation, the empirical formulation can be a useful tool for evaluating stress concentration factors without going through complex numerical calculations or expensive finite element modeling. The empirical formulation in its present form only deals with equally sized cavities, but these cavities are often of different sizes in actual die castings. Therefore, the empirical formulation should be modified to account for an unequally sized cavity pair for better application to practical situations.

Table 5
Comparison of parameters obtained from exclusive and coupled search methods.

	Parameters	Exclusive method	Coupled method
Cosine – power function	ξ	1.9472	1.8680
	η	0.5740	0.6440
Cosine-exponential function	t_1	0.0065	0.0095
	t_2	0.0863	0.1205
	B_1	3.1692	3.0700
	B_2	1.0743	1.0000
	ξ	1.9472	1.8780

Although both of the formulations presented in this paper can accurately predict the stress concentration factors over a wide range of inter-cavity separations and orientations, they overestimate the stress concentration that would arise in actual components containing very closely spaced cavities. In such cases, in which the cavity boundaries almost touch each other, the power formulation in Eq. (7) would predict a stress concentration factor of infinity, while the double exponential formulation in Eq. (9) gives rise to a stress concentration factor of 5.89.

A quantitative comparison of parameters obtained by exclusive and coupled search method has been presented in Table 5, both for single power and double exponential function. Both exclusive and coupled approach yield parametric values quite close to each other. Mathematically any of the chosen functions, single power or double exponential, fit the simulation data quite well. Selecting a function should be based on practical application. Depending on external loading, the material may yield before attaining such high stress concentrations. It should be noted that the double exponential formulation has a better predictive capability than the power law formulation for closely spaced cavities, as the prediction converges to a relatively reasonable finite value that could occur under low loading conditions. There is also inaccuracy in predicting stress concentration factors using empirical formulae for cavity pairs whose inter-cavity axis is oriented at a high angle to the loading direction, especially for an orientation angle 90° and a closely separated cavity pair. In such situations, the empirical formulation overestimates the K_t values by about 10%. Such level of overestimation is not so critical and the slight decrease in stress concentration factor at 90° is not important to evaluate the strength of materials. Moreover, the probability of 90° alignment of closely separated cavities is very low in practical situations. Therefore, the empirical formulation is probably acceptable from a practical perspective. Alternatively, one may employ the K_t of an isolated cavity instead of using the empirical formula, neglecting the interaction effect when there is a high orientation angle. In this study although we have formulated empirical function of dual cavity system, in practical case of die cast materials there are many cavities. So the effect of multi-cavities on stress concentration factor cannot be neglected. However, we can guess the closest neighbor cavities are the most dangerous and important but the stress relief by vertical orientation should not be neglected.

6. Conclusions

Extensive finite element analysis was carried out to understand the effects of various parameters on the stress concentration factor for a pair of spherical cavities. Two empirical formulae are proposed, which take into account parameters such as the relative separation distance between the cavities and the angle between the inter-cavity axis and the loading direction. Both of the formulations can accurately predict the stress concentration factors, except when the cavities are very closely spaced. The single power function represents an ideal elastic stress analysis, while the double exponential function is more realistic especially when the cavities are very close to each other. The double exponential formulation has a better predictive capability for closely spaced cavities and under low loading. For orientation angles below 45° and for inter-cavity separations δ of less than 1.2, there is strong interaction between the cavities. These simple empirical formula are useful in deciding which particular gas pores in an aluminum die cast would be critical from a stress concentration point of view, and can therefore be used as a tool to predict fatigue crack initiation. In future work, the empirical formulae will be modified to take into account gas pores of unequal size.

Acknowledgements

This research was financially supported by the Suzuki Foundation and JSPS KAKENHI (20710057).

References

- [1] C.M. Sonsino, J. Ziese, Fatigue strength and application of cast aluminum alloys with different degrees of porosity, *Int. J. Fatigue* 15 (1993) 75–84.
- [2] J.M. Boileau, J. Allison, The effect of porosity size on fatigue properties in a cast 319 aluminium alloy, *SAE Trans.* (2001) 648–659.
- [3] O. Kuwazuru, Y. Murata, Y. Hangai, T. Utsunomiya, S. Kitahara, N. Yoshikawa, X-ray CT inspection for porosities and its effect on fatigue of die cast aluminum alloy, *J. Solid Mech. Mater. Eng.* 2 (2008) 1220–1231.
- [4] R.A. Hardin, C. Beckermann, Prediction of the fatigue life of cast steel containing shrinkage porosity, *Metall. Mater. Trans. A* 40 (2009) 581–597.
- [5] Y. Lu, F. Taheri, M.A. Gharghoury, H.P. Han, Experimental and numerical study of the effect of porosity on fatigue crack initiation of HPDC magnesium AM60B alloy, *J. Alloys Compd.* 470 (2009) 202–213.
- [6] B. Skallerud, T. Iveland, G. Harkegard, Fatigue life assessment of aluminum alloys with casting defects, *Eng. Fract. Mech.* 44 (1993) 857–874.

- [7] M.J. Couper, A.E. Neeson, J.R. Griffiths, Casting defects and the fatigue behavior of an aluminum casting alloy, *Fatigue Fract. Eng. Mater. Struct.* 13 (1990) 213–227.
- [8] M.A. Sadowsky, E. Sternberg, Stress concentration around an ellipsoidal cavity in an infinite body under arbitrary plane stress perpendicular to the axis of revolution of cavity, *J. Appl. Mech.* 14 (1947) 191–201.
- [9] E. Sternberg, M.A. Sadowsky, On symmetric problem of the theory of elasticity for an infinite region containing two spherical cavities, *J. Appl. Mech.* 19 (1952) 19–27.
- [10] H. Miyamoto, On the problem of theory of elasticity for a region containing more than two spherical cavities, *Bull. JSME* 1 (1958) 103–108.
- [11] R.A. Eubank, Stress interference in three dimensional torsion, *J. Appl. Mech. Trans. ASME* 25 (1965) 21–25.
- [12] E. Tsuchida, I. Nakahara, On symmetric problem of elasticity theory for an infinite elastic solid containing some spherical cavities, *Bull. JSME* 19 (1976) 993–1000.
- [13] H. Cheng, A. Acrivos, The solution of the equations of linear elasticity for an infinite region containing two spherical inclusions, *Int. J. Solids Struct.* 14 (1978) 331–348.
- [14] H.R. Sadraie, S.L. Crouch, S.G. Mogilevskaya, A boundary spectral method for elasto-static problems with multiple spherical cavities and inclusions, *Eng. Anal. Boundary Elem.* 31 (2007) 425–442.
- [15] D. Lukic, A. Prokic, P. Anagnosti, Stress-strain field around elliptical cavities in elastic continuum, *Eur. J. Mech. A/Solids* 28 (2008) 86–93.
- [16] S. Bidhar, O. Kuwazuru, Y. Hangai, T. Utsunomiya, N. Yoshikawa, Empirical prediction of stress concentration factor for a pair of spherical cavities, in: 4th International Conference on Modeling Simulation and Optimization, Malaysia, April 19–21, 2011, paper no. 83874.
- [17] <https://www1.ansys.com/customer/default.asp>.
- [18] J.N. Goodier, Concentration of stress around spherical and cylindrical inclusions and flaws, *ASME J. Appl. Mech.* 5 (1933) 39–44.
- [19] S. Timoshenko, *Theory of Elasticity*, McGraw-Hill, New York, USA, 1951. pp. 359–362.
- [20] Z.R. Li, C.W. Lim, L.H. He, Stress concentration around a nano-scale spherical cavity in elastic media: effect of surface stress, *Eur. J. Mech. A/Solids* 25 (2006) 260–270.
- [21] S.G. Lekhnitski, *Theory of Elasticity of an Anisotropic Body*, MIR publishing, Moscow, Russia, 1981. pp. 404–410.
- [22] Chun.-Ron. Chiang, Stress concentration factors of a general tri-axial ellipsoidal cavity, *Fatigue Fract. Eng. Mater. Struct.* 31 (2008) 1039–1046.
- [23] R.G.D. Steel, J.H. Torrie, *Principles and Procedures of Statistics*, McGraw-Hill, New York, 1960.
- [24] http://en.wikipedia.org/wiki/Coefficient_of_determination.